

MethaneSAT data analysis of oil and gas methane emissions from California's San Joaquin basin

James P. Williams¹, Katlyn MacKay¹, Marvin Knapp^{1,2}, Joshua Benmergui^{1,2}, Anthony Himmelberger¹, Mark Omara¹, Jack Warren¹, Kaiya Weatherby¹, Ben Lyke¹, Steven Wofsy², Ritesh Gautam¹

¹MethaneSAT LLC and Environmental Defense Fund

²Harvard University

Eight MethaneSAT scenes were analyzed over California's San Joaquin basin between September 2024 and May 2025. In terms of oil and gas production, this region is oil-dominant, with ~83% of total marketed energy production in 2024 coming from oil. Based on a spatiotemporal aggregation of the MethaneSAT observations, the total oil and gas methane emissions are estimated at 18 (95% confidence interval: 12 – 26) tonnes per hour (t/h), representing a methane intensity of 8.9% (95% confidence interval: 5.6% – 12.4%) relative to marketed gas production and 0.27 (95% confidence interval: 0.17 – 0.37) kg of methane per gigajoule (GJ) of total energy production (Fig. 1). Estimated methane intensity is elevated and may reflect the prevalence of fugitive emissions from low producing oil wells in the region (Williams et al. 2025).

MethaneSAT detected emission hotspots in the south of the observed San Joaquin region align with areas of oil and gas production. Significant methane sources not associated with oil and gas are present throughout the observed region, notably from agriculture (livestock operations) and landfills, which align with hotspots in the northern part of the region. Total MethaneSAT regional methane emissions (142 t/hr, 95% confidence interval: 104 – 181) are about 2× greater than the [gridded EPA inventory](#) for the year 2020 (the most recent available, see Fig. 2). The EDGAR 2024 emissions inventory estimates are roughly 2.2× the MethaneSAT total (Fig. 2).

Methane emissions are quantified from MethaneSAT's retrieved column averaged mole fractions of methane (X_{CH_4}) using a Bayesian atmospheric inversion framework (The MethaneSAT Science and Engineering Team, 2026), which generates the MethaneSAT Level-4 gridded emissions product (at 4 km × 4 km resolution). We attribute MethaneSAT derived methane emissions to sectors by combining information from bottom-up inventories and satellite-detected point sources using proportional allocation. We assess oil and gas methane intensity using two distinct and complementary metrics: 1) Marketed gas-production-normalized methane intensity (Eq. 1) and 2) Marketed oil-and-gas-normalized methane intensity (Eq. 2). MethaneSAT emissions data product and inversion methods, sectoral disaggregation, and methane intensity calculations are described in Williams et al. 2025.

Methane intensity calculations-

$$CH_4 \text{ intensity}_{gas}(\%) = \left(\frac{E_{ong}}{P_{gas} \times CH_4_{comp.}} \right) \times 100 \quad (\text{Eq. 1})$$

$$CH_4 \text{ intensity}_{energy}(kgCH_4/GJ) = \left(\frac{E_{ong}}{P_{ong}} \right) \quad (\text{Eq. 2})$$

E_{ong} = MethaneSAT derived oil and gas methane emissions

P_{gas} = Marketed gas production in 2024

P_{ong} = Marketed oil and gas production in 2024

$CH_4_{comp.}$ = Methane composition of natural gas, assumed to be 90% for marketed gas

Methane density = 0.0192 kg/ft³
 1 boe = 6000 ft³ natural gas, 1 boe = 5.710 GJ

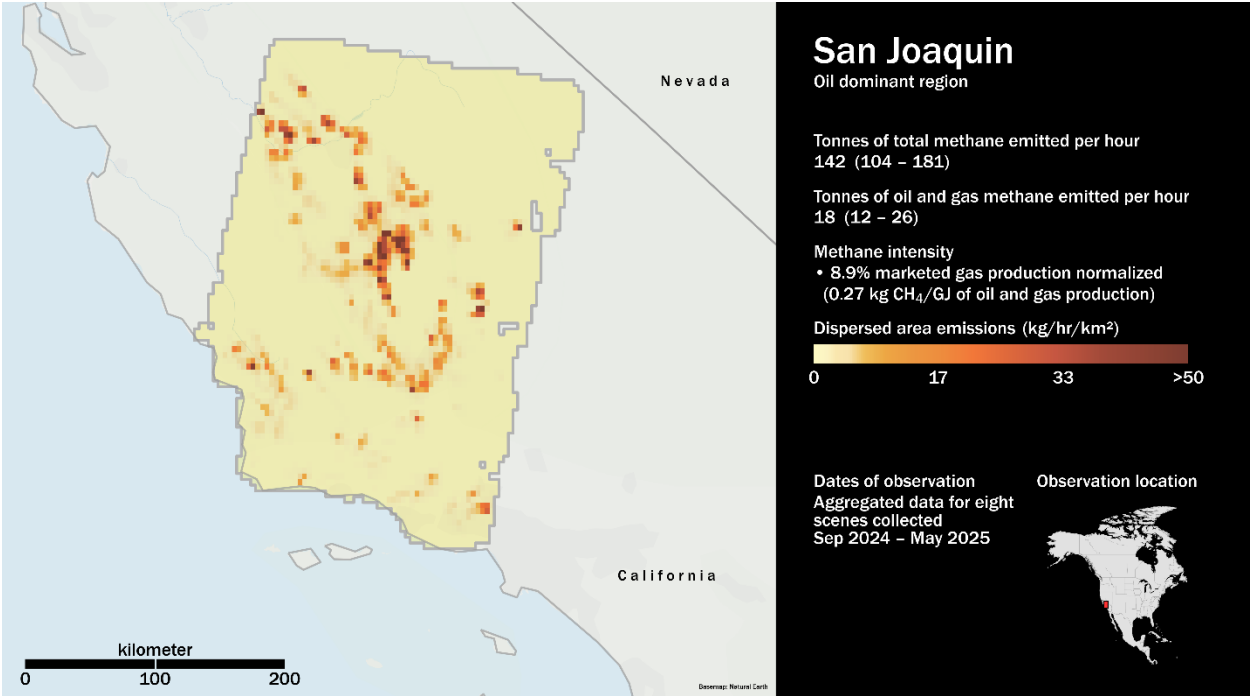


Figure 1: An aggregated heatmap of methane emission rates (kg/hr/km²) produced by MethaneSAT observations over the San Joaquin basin in California, based on an aggregation of eight unique observations collected between September 2024 and May 2025. MethaneSAT derived total methane emission rates and oil/gas methane emission rates with uncertainties are noted, along with methane intensity.

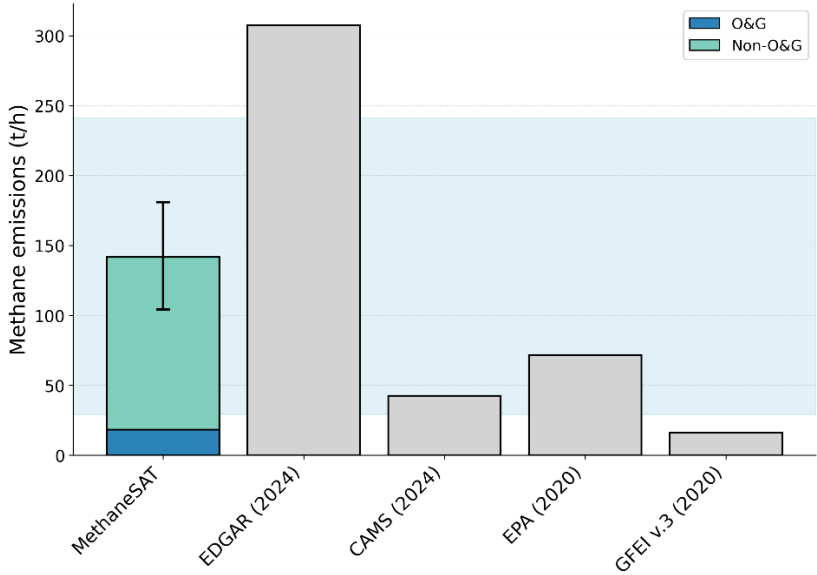


Figure 2: MethaneSAT total emissions compared to bottom-up inventories. The shaded blue area is the bootstrapped 95% confidence interval of previous estimates. Note that GFEIv3 is for oil, gas and coal methane emissions only. The year of emissions estimates are shown in parenthesis.

References:

Soulie, A., Granier, C., Darras, S., Zilbermann, N., Doumbia, T., Guevara, M., Jalkanen, J.-P., Keita, S., Lioussé, C., Crippa, M., Guizzardi, D., Hoesly, R., and Smith, S. J.: Global anthropogenic emissions (CAM5-GLOB-ANT) for the Copernicus Atmosphere Monitoring Service simulations of air quality forecasts and reanalyses, *Earth Syst. Sci. Data*, 16, 2261–2279, <https://doi.org/10.5194/essd-16-2261-2024>, 2024.

Crippa, M., Guizzardi, D., Pagani, F., Banja, M., Muntean, M., Schaaf, E., Quadrelli, R., Riquez Martin, A., Taghavi-Moharamli, P., Köykkä, J., Grassi, G., Melo, J., Suárez-Moreno, M., Sedano, F., San-Miguel, J., Manca, G., Pisoni, E., and Pekar, F.: GHG emissions of all world countries: 2025, Publications Office of the European Union, 2025.

Maasackers, J. D., McDuffie, E. E., Sulprizio, M. P., Chen, C., Schultz, M., Brunelle, L., Thrush, R., Steller, J., Sherry, C., Jacob, D. J., Jeong, S., Irving, B., and Weitz, M.: A Gridded Inventory of Annual 2012–2018 U.S. Anthropogenic Methane Emissions, *Environ. Sci. Technol.*, 57, 16276–16288, <https://doi.org/10.1021/acs.est.3c05138>, 2023.

Scarpelli, T. R., Roy, E., Jacob, D. J., Sulprizio, M. P., Tate, R. D., and Cusworth, D. H.: Using new geospatial data and 2020 fossil fuel methane emissions for the Global Fuel Exploitation Inventory (GFEI) v3, *Earth Syst. Sci. Data*, 17, 7019–7033, <https://doi.org/10.5194/essd-17-7019-2025>, 2025.

The MethaneSAT Science and Engineering Team: MethaneSAT Level-4 Dispersed Emissions Product: Algorithm Theoretical Basis Document v1.1, <https://doi.org/10.5281/zenodo.19873046>, 2026.

Williams, J. P., Benmergui, J., Knapp, M., Omara, M., Himmelberger, A., Kyzivat, E., Weatherby, K., Lyke, B., Warren, J., MacKay, K., Ayvazov, S., Russi, M., LoFaso, N., Melendez, T., Miller, C. C., Roche, S., Sargent, M., Franklin, J., Nasr, M., Zhang, Z., Miller, D. J., Luo, B., Guanter, L., Hamburg, S. P., Wofsy, S. C., and Gautam, R.: Methane intensity and emissions across major oil and gas basins and individual jurisdictions using MethaneSAT observations, *Atmos. Chem. Phys.*, 26, 5961–5981, <https://doi.org/10.5194/acp-26-5961-2026>, 2026.